Electronic Supplementary Information

Syntheses, Structures and Properties of 5-Azotetrazolyl Salicylic Acid and Its Dilanthanide Complexes

Wen-Bin Chen,[a] Zhi-Xin Li,[a] Xin-Wei Yu,[a] Meng Yang,[a] Yan-Xuan Qiu,[a] Wen Dong,*[,a] and Ya-Qiu Sun*[,b]

[a]School of Chemistry and Chemical Engineering, Guangzhou Key Laboratory for Environmentally Functional Materials and Technology, Guangzhou University, Guangzhou 510006, P. R. China

[b]Department of Chemistry, Tianjin Normal University, Tianjin 300383, P. R. China

Electronic Supplementary Information – Table of Contents

Powder X-ray diffraction

Powder X-ray diffraction (XRD) data were collected on a Rigaku/max-2550 diffractometer with Cu-Kα radiation (λ = 1.5418 Å). The simulated and experimental P-XRD patterns of **3**–**7** are shown in Fig. S1. Their peak positions are in good agreement with each other indicating the phase purity of the samples used in the physical measurements.

TD-DFT calculations for the absorption spectra of the alkaline aqueous solution of 1

In order to gain a better understanding for the absorption spectra of the alkaline aqueous solution of **1** and the photoisomerization reaction, TD-DFT was employed to obtain insight into the electronic structures of the trans-enol-E and cis-enol-E isomers of ASA^{3-} anion. Fig. S7 shows state energy diagrams for the trans-enol-E and the optimized cis-enol-E isomer of ASA^{3-} anion. The calculated first main electronic absorption for the trans-enol-Z of of ASA^{3-} anion is HOMO-1→ LUMO transition with oscillator strength f = 0.5614 which originates from the salicylic π (80.28 to 38.53% contributors) to azo n* (10.47 to 51.39% contributors) and tetrazolate π* (9.25 to 10.08% contributors) transition, and the electronic transition energy of 2.8585 eV corresponds to a maximum absorption peak of around 434 nm (Fig. S7a). The second electronic transition with an oscillator strength of f = 0.0467 and the electronic transition energy of 4.3320 eV corresponding to absorption peak of around 286nm is attributed to the HOMO→ LUMO+2 transition that originates from salicylic π (97.41 to 78.35% contributors) to azo n* (1.10 to 6.53% contributors) and tetrazolate π* (1.49 to 15.12% contributors) transition (Fig. S7b). For cis-enol-E ASA^{3-} former, the calculated first electronic absorption with oscillator strength f = 0.0925 is attributed to the HOMO→ LUMO+1 transition that originates from salicylic π (89.56 to 88.42% contributors) and azo n (8.43 to 1.22% contributors) to tetrazolate π* (2.01 to 10.36% contributors) transition, and the electronic transition energy of 3.5214 eV corresponds to a maximum absorption peak of around 355 nm (Fig. S7c). The second electronic transition with an oscillator strength of f = 0.3644 and the electronic transition energy of 4.9794 eV corresponding to absorption peak of around 249 nm is attributed to the HOMO-10→ LUMO transition that originates from salicylic π (46.73 to 15.29% contributors) and tetrazolate π (42.52 to 23.36% contributors) to azo n* (10.75 to 61.35% contributors) transitions (Fig. S7d). Based on the above DFT calculation, the maximum absorption peak transfer from 445 to 355 nm under 365 nm UV light irradiation should originate from trans-enol to cis–enol photoisomerization reaction of ASA^{3-} anion (Scheme 1). However, it is difficult to demonstrate the photochromism for the solid samples and E-Z transfer in solution using TD-DFT calculation and the work should be paid to the further research.

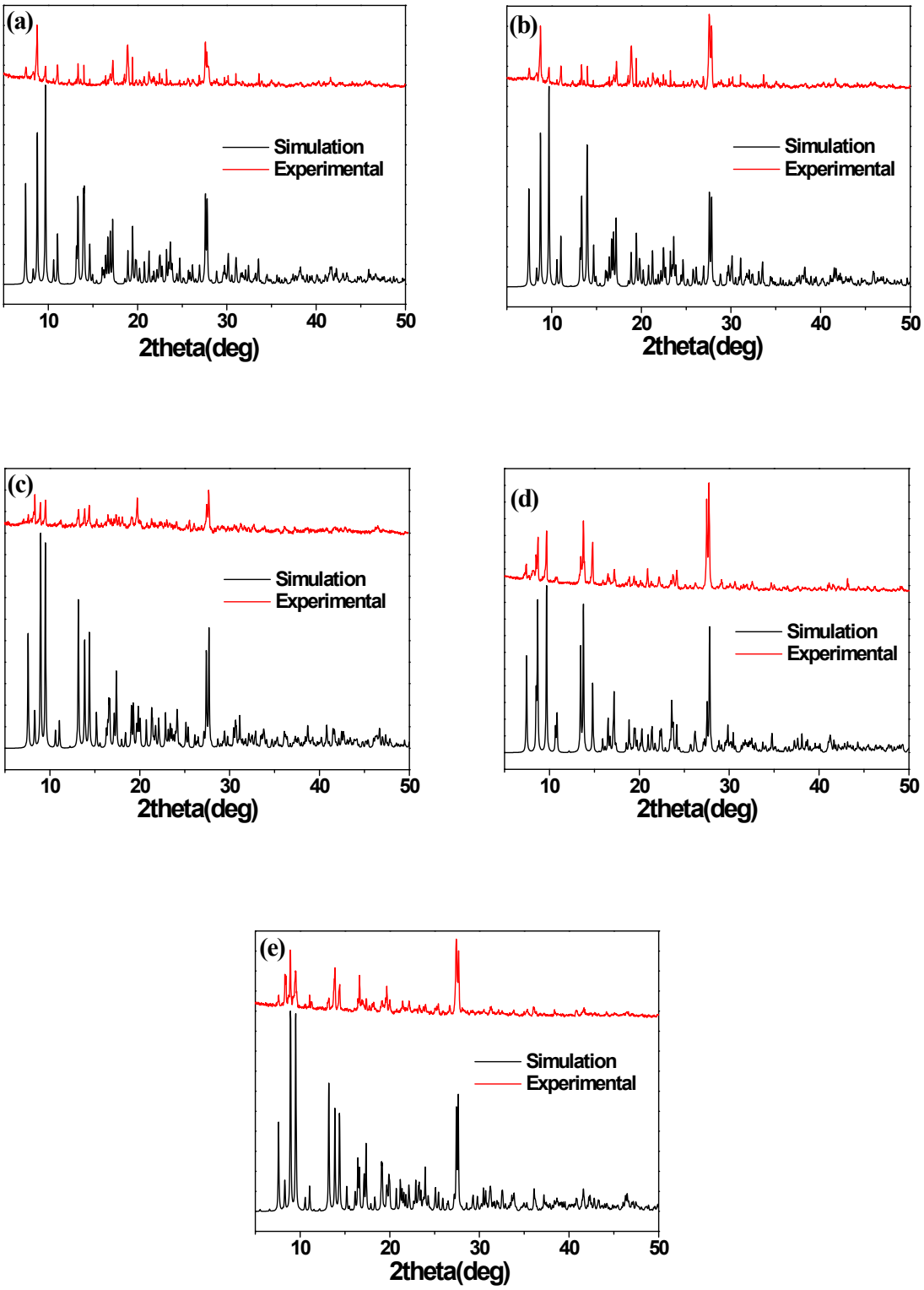

Fig. S1. (a)-(e) X-ray powder diffraction patterns for **3-7,** respectively.

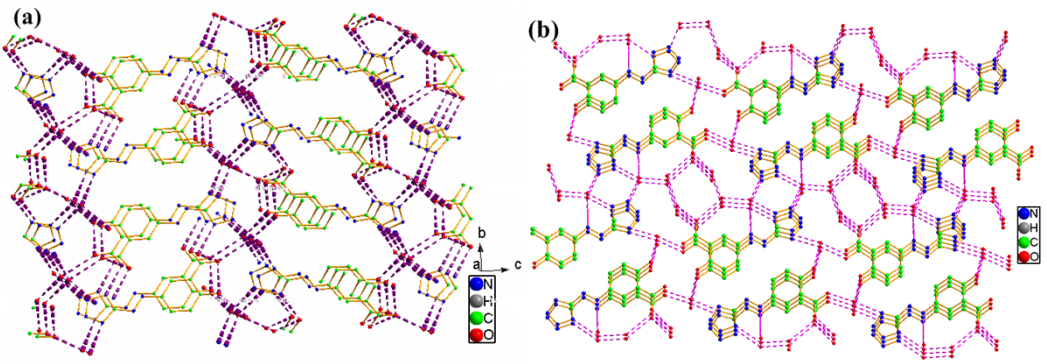

Fig. S2. (a) (b) 3D supramolecular structure of **1** and **2**, respectively.

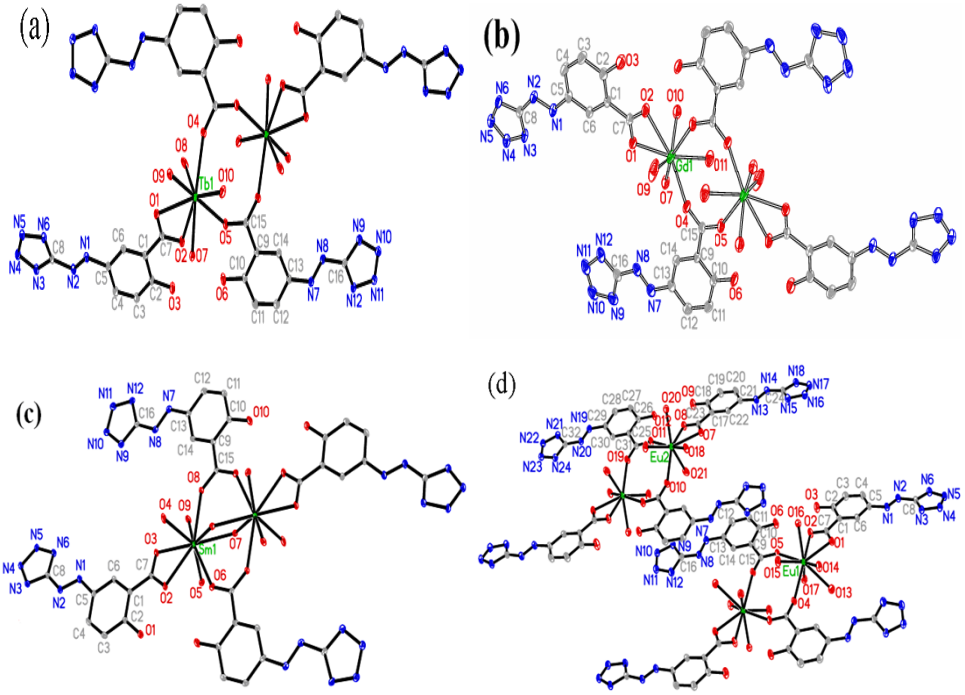

Fig. S3. (a), (b), (c) and (d) The atomic labeling diagram of **4**-**7**, respectively. All H atoms and lattice water molecules have been omitted for clarity.

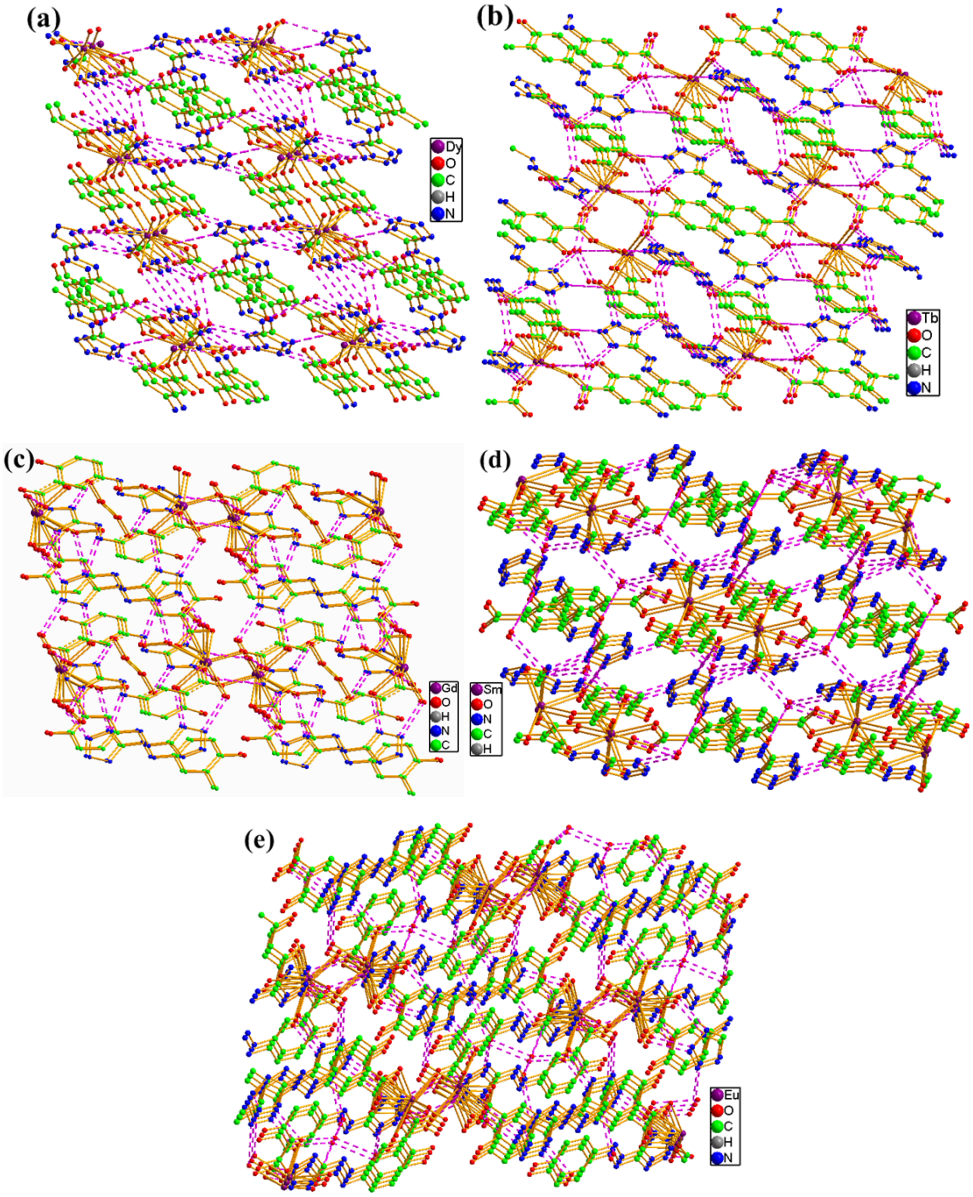

Fig. S4. (a)-(e) 3D supramolecular structure of **3**-**7**, respectively.

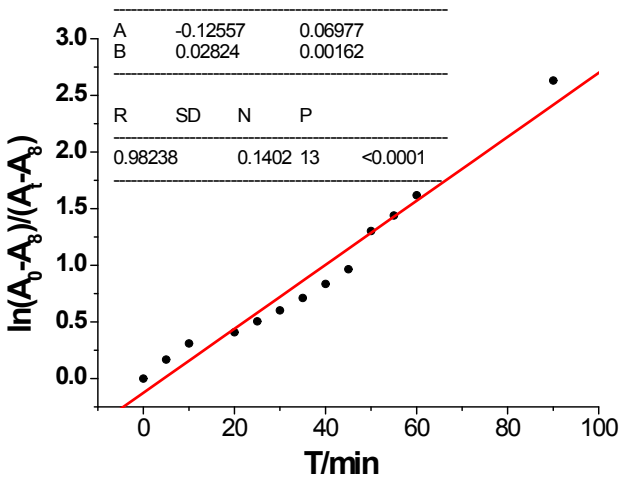

Fig. S5. Photoisomerization of **1** $\ln((A_0-A_\infty)/(A_t-A_\infty)) = A+Bt$; $B = 2.824\times10^{-2}$ min^{-1}.

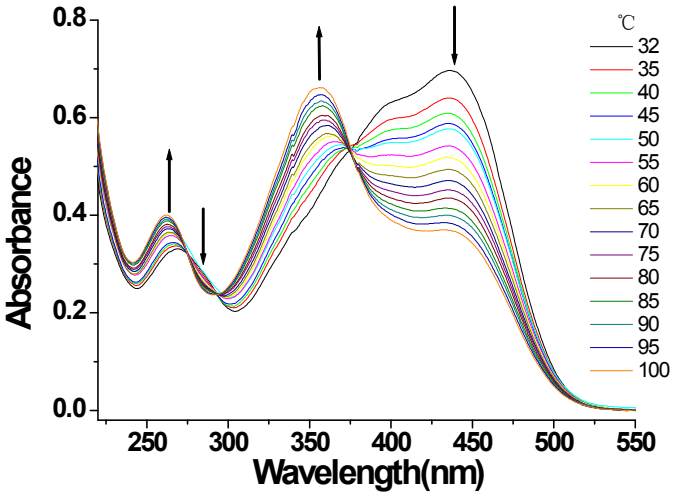

Fig. S6. The temperature-dependent changes of UV-vis absorption spectra of aqueous solutions of **1** with concentration of $5x10^{-5}$ mol·dm^{-3} and pH = 11.64 in the temperature range of 32-100 °C.

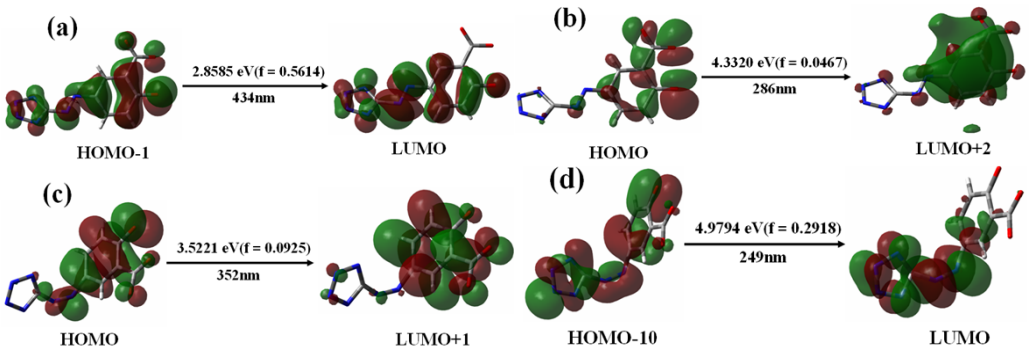

Fig. S7. (a), (b) State energy diagrams and contributing molecular orbitals for trans-enol-E of ASA^{3-}; (c), (d) State energy diagrams and contributing molecular orbitals for the optimized cis-enol-E isomer of ASA^{3-}.

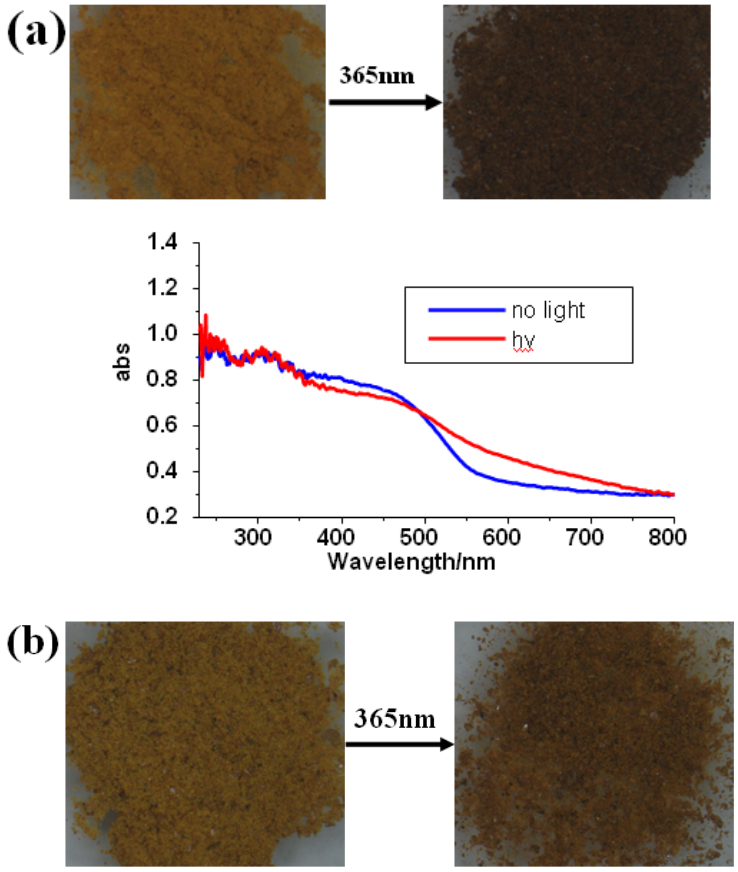

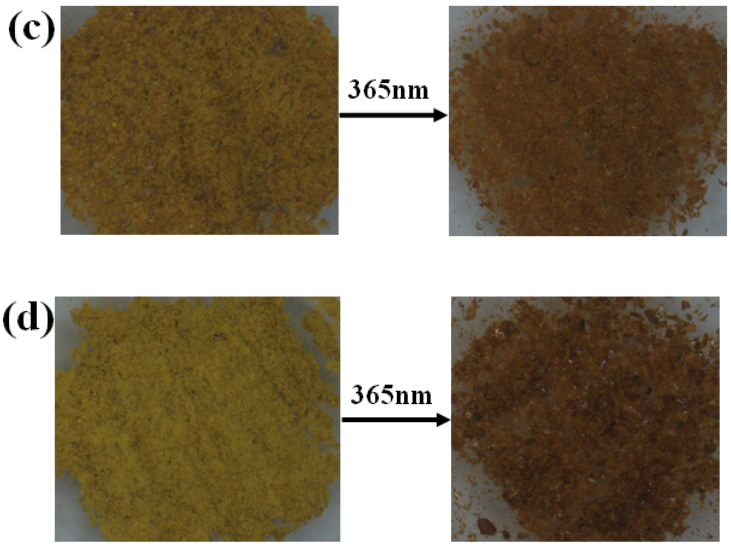

Fig. S8. (a) The color and the corresponding to diffuse reflectance spectra for the powder samples of **4**. (b), (c) and (d) The color changes of the crystal powder samples of **5**–**7**, respectively.

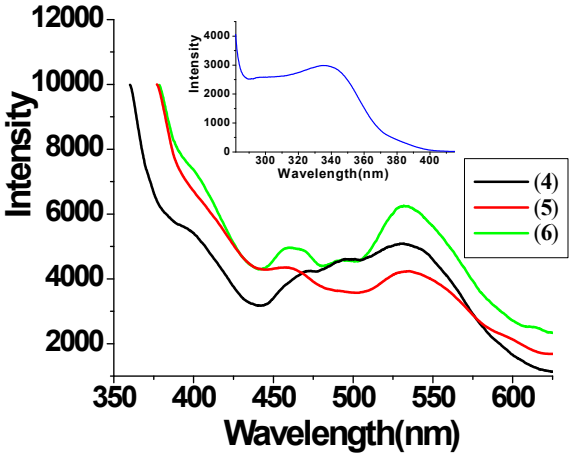

Fig. S9. The emission spectra of **5**–**7** (inset is Excitation spectrum).

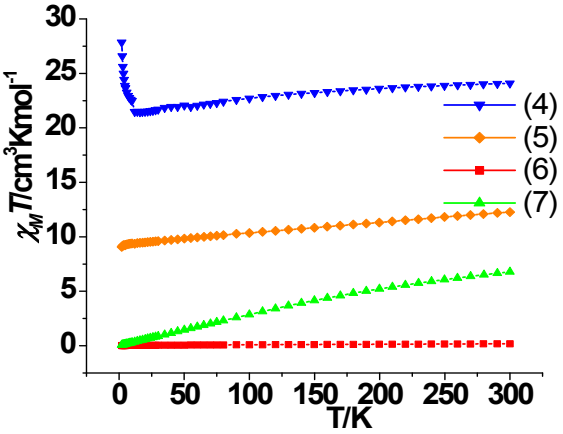

Fig. S10. The plot of $\chi_M T$ versus T for **4-7** in the magnetic field of 1000 Oe in 2–300 K.

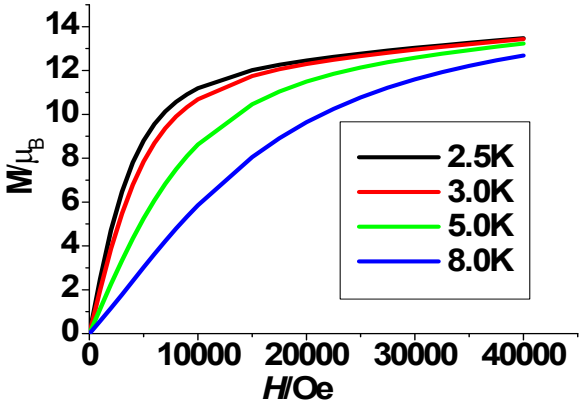

Fig. S11. M versus H plots in the field range 0–40 kOe for **3**.

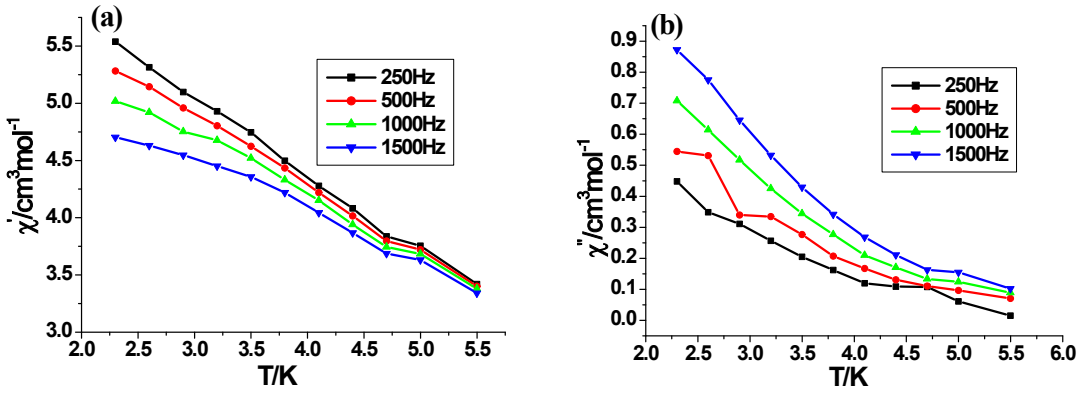

Fig. S12. (a) and (b) Temperature-dependence of the in-phase (χ′) and out-of-phase (χ′′) of ac susceptibility of **3** at 250-1500 Hz.

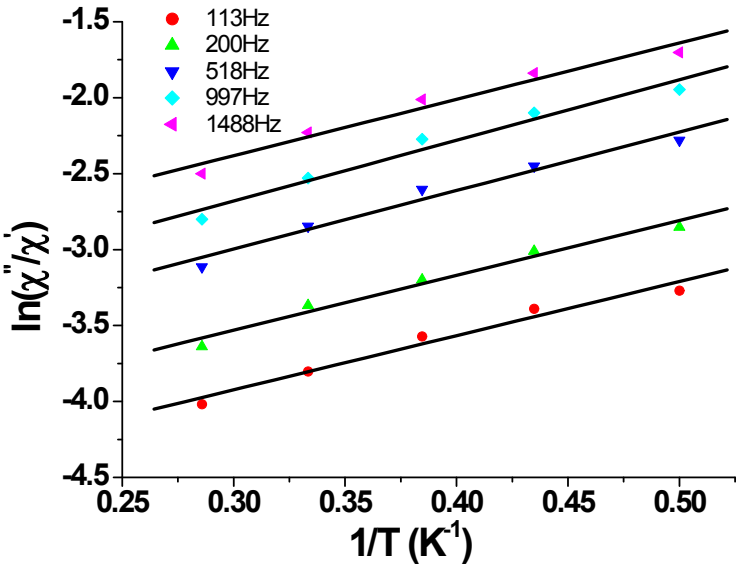

Fig. S13. Natural logarithm of the ratio of χ''over χ' versus $1/T$ of the data for **3**.

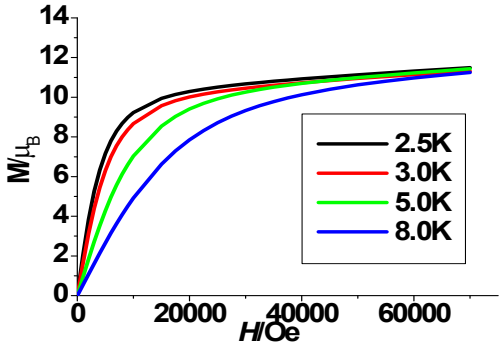

Fig. S14. M versus H plots in the field range 0–70000 Oe for **4**.

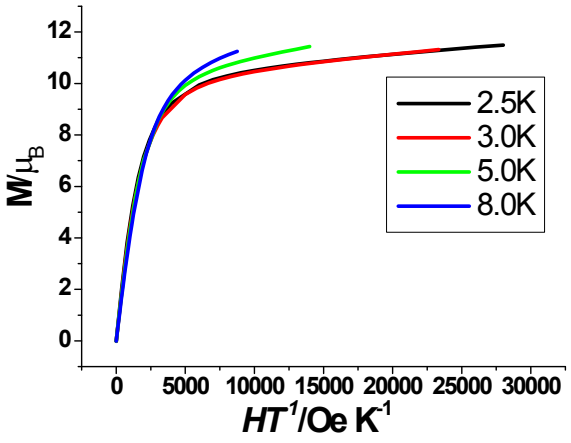

Fig. S15. M versus H/T plots in the field range 0–70000 Oe for **4**.

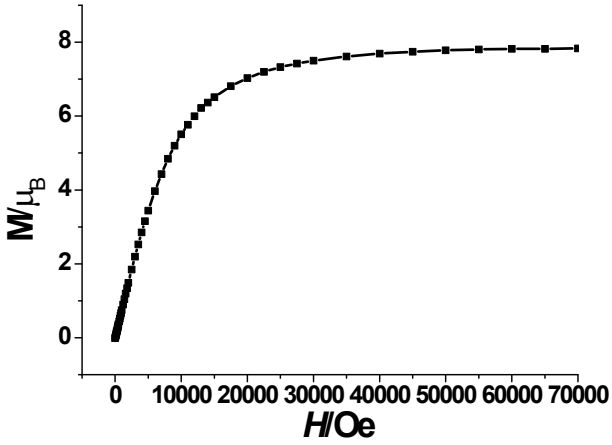

Fig. S16. M versus H plots in the field range 0–70000 Oe at 2K for **5**.

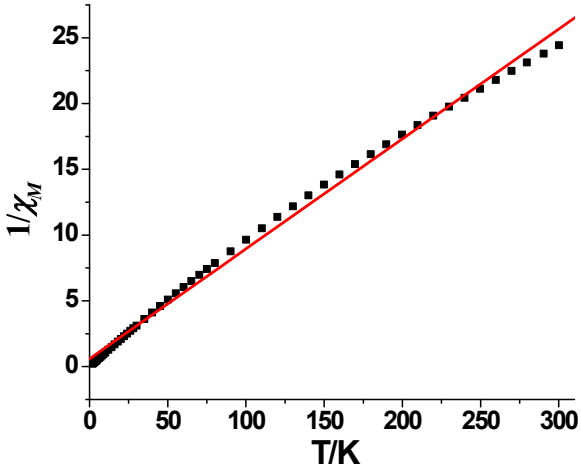

Fig. S17. The $1/\chi_M$ versus T plot in the range from 300 to 2 K for **5**.

Table S1 Cartesian coordinates for tran-enol isomer of H_3ASA

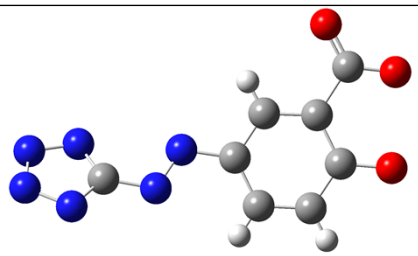

N	4.87520000	3.87970000	3.52910000
N	6.01800000	4.02280000	4.05530000
N	6.82420000	4.89470000	1.91570000
N	8.28600000	4.11450000	3.36240000
N	8.06040000	5.02560000	1.42340000
N	8.93620000	4.54740000	2.27100000
C	2.65420000	3.13180000	3.87590000
H	2.60920000	3.02450000	2.95440000
C	3.82250000	3.61270000	4.44050000
C	2.81700000	3.49740000	6.59740000
H	2.86410000	3.62940000	7.51700000
C	1.63890000	2.99180000	6.03750000
C	1.54910000	2.80540000	4.64880000
C	3.90080000	3.80140000	5.81890000
H	4.68050000	4.12970000	6.20550000
C	7.00680000	4.31950000	3.11680000
C	0.30600000	2.25680000	4.02530000
O	0.60390000	2.69850000	6.83850000
O	-0.68910000	2.09810000	4.78210000
O	0.30350000	2.00490000	2.80730000

Table S2 Cartesian coordinates for cis-enol isomer of H_3ASA.

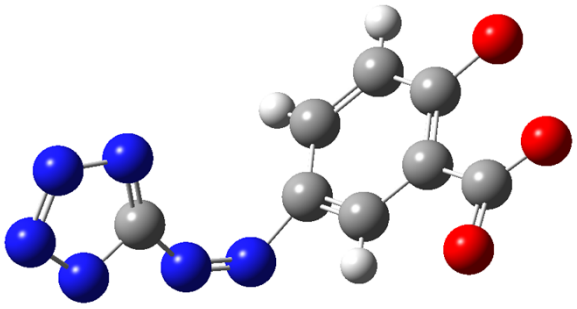

N	2.30923647	4.12831558	-2.27819836
N	3.05497933	3.13607471	-2.09689041
N	5.70353469	3.14551970	-1.83257315
N	4.32889781	1.49542957	-1.93535211
N	5.53434235	1.02522694	-1.66240523
N	6.39639737	2.01902294	-1.65309633
C	3.69108196	7.08446283	-5.67553230
C	3.40904939	7.73044711	-1.96851472
H	3.56810284	8.42261156	-1.36813252
C	2.96094107	6.51794684	-1.50354418
H	2.80688574	6.39203755	-0.59447697
C	3.40936237	6.88234648	-4.23475219
C	3.62757841	7.93041440	-3.32798780
C	2.95224203	5.66835896	-3.75377973
H	2.78860885	4.97362988	-4.34902298
C	4.40914609	2.78698705	-1.94199992
C	2.73652997	5.47386975	-2.40402650
O	4.02531619	8.17913422	-6.12252986
O	3.57610065	6.00885136	-6.39167706
O	4.03765817	9.15568844	-3.73122990